

EROS/MACHO Gravitational Microlensing Events Toward LMC in Evans Halo Model

Sohrab Rahvar*

Department of Physics, Sharif University of Technology,
P.O.Box 11365–9161, Tehran, Iran
Institute for Studies in Theoretical Physics and Mathematics,
P.O.Box 19395–5531, Tehran, Iran

December 19, 2018

Abstract

After a decade of gravitational microlensing experiments, 13 to 17 events by MACHO (depending on quality) and two events by EROS have been detected. All of those have been observed in the direction of Large Magellanic Cloud. We use Evans spherically symmetric halo model to study the rate of microlensing events. The expected number of events in this model obtain by using EROS and MACHO observational efficiencies. We compare our numbers with the observed events to obtain the fraction of halo that is made by compact objects. It is shown that results derived from two experiments are in good agreement with each other and MACHOs, comprise only a fraction (depending on the model) of Milky Way halo. The results are also compatible with the White Dwarfs population studies in the Hubble Deep Field.

1 Introduction

The existence of dark matter becomes apparent by studying the rotational curve of spiral galaxies [1] & [2]. Recent results of optical and 21 cm band observations shows that for thousands of spiral galaxies, the Keplerian rotational velocity beyond the luminous radius remains constant [3]. Diffusion emission in X-rays from elliptical galaxies and dynamics of cluster of galaxies also shows that there should exist a halo structure around spiral galaxies. Various dark matter candidates such as, baryonic dark matter and exotic dark candidates such as Axions, massive neutrinos, WIMPs and Super-symmetric particles have been proposed. However, simulations show that there is a discrepancy between expected rotational velocity due to cold dark matter of halo and observed velocity curves [4] & [5].

In the case of baryonic dark matter, Big Bang nucleosynthesis models give $\Omega_B h^2 = 0.02$ [6] & [7] while measuring the mass of luminous stars obtain Ω_{lum} of universe to be around 0.004 [8]. Comparing Ω_B with Ω_{lum} ($\Omega_B \gg \Omega_{lum}$), provides an other

*E-mail:rahvar@mehr.sharif.edu

evidence for the existence of baryonic dark matter. One of the types of baryonic dark matter could be in the form of Massive Astrophysical Compact Halo Objects (MACHO). These objects due to their light masses are obscure. Neutron stars and black holes as dark objects can also be considered in this category. The pioneer work of using gravitational microlensing technique for detection of compact objects was proposed by Paczyński [9]. Since his proposal, microlensing searches have turned very quickly into reality and some groups like AGAPE, DUO, EROS, MACHO, OGLE and PLANET have contributed to this field. After one decade, the final results of experiments compared with the theoretically expected results, provides a constraint on the fraction of halo in the form of compact objects. This results strongly depends on the galactic model and mass function of MACHOs. Using the standard model for Milky Way and delta mass function for MACHOs, EROS and MACHO groups could obtain the fraction of halo that is made of compact objects. EROS result, puts a strong constraint on the fraction of halo made of objects in the range $[10^{-7}M_{\odot}, 4M_{\odot}]$, excluding at 95% C.L. that more than 40% of the standard halo is made of objects with up to one solar mass [11]. The analysis of 5.5 years observation of LMC by the MACHO group estimates that the halo mass fraction in the form of compact halo objects is about 20% [12].

Here, we use the most general spherically symmetric model for the halo of spiral galaxies that interprets Keplerian rotational curves[10]. The expected distribution of gravitational microlensing events obtain by applying the efficiency of EROS and MACHO experiments in these models. Here we use power law mass function for the compact halo objects and mass function of disk derived from HST observation. We compare the expected rate of events with those observed experimentally to evaluate the fraction of halo made by MACHOs.

The organization of the paper is as follows. In Sect. 2, we introduce the basics of gravitational microlensing and obtain relation between the optical depth and the rate of microlensing events. In Sect. 3 we introduce Evans model for galactic structure and in Sect. 4 we estimate by Monte-Carlo simulation the expected rate of microlensing events toward LMC in six different galactic models. We then calculate the fraction of halo made by MACHO in different models. The results are discussed in Sect. 5.

2 Basics of gravitational microlensing

In this section we present the main feature of gravitational microlensing and in particular, we obtain relation between optical depth and the rate of events. For review, see ([13], [14], [15], & [16]).

According to general relativistic results, a given light ray bends near a massive star. Considerable gravitational lensing occurs when the line of sight between us and a background star passes near enough a lens. Since the deflection angle in the case of microlensing is too small (taking into account the resolution of present apparatus), it is impossible to distinguish two images that are produced due to the gravitational lensing, thus the effect is only on the brightness magnification of the background star. This magnification is given by

$$A(t) = \frac{u(t)^2 + 2}{u(t)\sqrt{u(t)^2 + 4}}, \quad (1)$$

where $u(t)^2 = u_0^2 + \left(\frac{t-t_0}{t_E}\right)^2$ is the impact parameter, normalized by Einstein Radius

$$R_E^2 = \frac{4GM D_{os}}{c^2} x(1-x). \quad (2)$$

In the definition of Einstein radius, D_{ol} and D_{os} are the distance of the lens and source from the observer and x is the fraction of these two terms, ($x = \frac{D_{ol}}{D_{os}}$). Definition of an event is given by constraint on maximum magnification with $A_{max} > 1.34$ or in other word $u < R_E$.

One of the crucial relation in statistical analysis of microlensing experiments is between the optical depth and the rate of events. Taking a snapshot from the background stars, the probability of existence the projected background stars inside Einstein Radius of lenses in the lens plane along our line of sight is the definition of optical depth. The optical depth of Microlensing event in the range of $[M, M + dM]$ can be obtain by:

$$d\tau(x; M, M + dM) = \frac{\pi R_E^2}{A} \left(\frac{\rho(x; M, M + dM)}{M} \right) \times (A \cdot dx). \quad (3)$$

$$d\tau(x; M, M + dM) = \frac{4\pi GM}{c^2} D_{os}^2 x(1-x) n(x) g(M) dM dx, \quad (4)$$

where, $dn = \frac{\rho(x; M, M + dM)}{M}$ is the number density of lenses in the range of $[M, M + dM]$ and can be written in the terms of mass function $g(M)$ and total density of compact object n_{total} as follows: $dn(M, M + dM) = n_{total} g(M) dM$, where the mass function is normalized to one. It is seen in Eq.(4) that optical depth is independent of mass function of MACHOs and it is only function of the density distribution of matter. The rate of events per year per the number of background stars Γ , as an observable quantity depends on the optical depth. The expected number of events in the range of $[M, M + dM]$ obtain:

$$dN_{exp}(x; M, M + dM) = \left(\frac{2R_E(x) \langle v_t(x) \rangle T_{obs}}{A(x)} \right) \times (n(x) g(M) dM \times A \cdot dx) \times N_{bg}, \quad (5)$$

where, T_{obs} and N_{bg} are the monitoring time and the number of background stars, $T_{obs} \times N_{bg}$ is called the exposure time and $\langle v_t(x) \rangle$ is the mean transverse velocity of lenses with respect to the line of sight. The mean transverse velocity obtain by velocity distribution function, $f_v(x)$ as follows:

$$\langle v_t \rangle = \int v_t(x) f_v(x) d^3 v, \quad (6)$$

where, the distribution function of velocity is normalized to one. The first term on the right hand side of Eq.(5) represents the ratio of spanned tube by a lens to the projection of background stars zone on the deflector plane, call it $A(x)$. The Second term denotes the number of lenses inside x and $x + dx$ and the last term shows the number of background stars. By definition of $d\Gamma = \frac{dN_{exp}(x)}{N_{bg} T_{obs}}$ and using Eq.(6), the rate of events is given by:

$$d\Gamma(x; M, M + dM) = 2(n(x) g(M) dM) R_E(x)^2 dx \int \frac{v_t(x) \epsilon(t_E)}{R_E(x)} f_v(x) d^3 v, \quad (7)$$

where, $\epsilon(t_E)$ is the efficiency of observation. By substituting Eq.(4) in Eq.(7) and using the definition of Einstein crossing time $t_E = \frac{R_E}{v_t}$, relation between the rate of

microlensing and the optical depth obtain as follows:

$$d\Gamma(x) = \frac{2}{\pi} d\tau \int \frac{f(x, v) \epsilon(t_E)}{t_E(x, v)} d^3v. \quad (8)$$

In the right hand side of Eq.(8), the value of integral is equal to the mean value of $\epsilon(t_E)/t_E$ ($f_x(v)$ is normalized to one). Rewriting Eq.(8) yields:

$$d\Gamma(x) = \frac{2}{\pi} d\tau(x) \left\langle \frac{\epsilon(t_E)}{t_E(x)} \right\rangle. \quad (9)$$

We take integral with respect to x , relation between rate of events and optical depth is given by:

$$\Gamma = \frac{2}{\pi} \tau \left\langle \frac{\epsilon}{t_E} \right\rangle. \quad (10)$$

Here, we are interested in to know the rate of events for a given optical depth. The theoretical rate of events ($\frac{d\Gamma}{dt_E}$) is available by a Monte-Carlo simulation based on the geometrical distribution of matter, velocity distribution and the mass function of lenses. The observational efficiency is also given as a function of event duration, depending on experimental setup and the strategy of observation. One can multiply these two distributions to estimate the expected number of microlensing events as follows:

$$\Gamma = \int \frac{d\Gamma}{dt_E} \epsilon(t_E) dt_E \quad (11)$$

In the next section we introduce different galactic models and obtain the expected rate and the total number of microlensing events toward Large Magellanic Cloud.

3 Galactic models

As mentioned in the last section, to calculate the rate of events, we need to know the density and velocity distributions and the mass function of lenses in the galactic model. The galactic structure falls into three different parts of the bulge, disk and halo. Our aim is to obtain the contribution of each part in the optical depth and the rate of events toward our line of sight (Large Magellanic Cloud). Since the contribution of the bulge on optical depth toward this direction is negligible, we ignore its contribution in our calculation. In what follows we consider the structure of disk and halo.

3.1 Galactic disk

The density profile of galactic disk can be given by a double exponential in cylindrical galactic coordinate system (R, z) as follows [17]:

$$\rho(R, z) = \frac{\Sigma_{\odot}}{2h} \exp \left[-\frac{R - R_{\odot}}{R_d} \right] \exp \left[-\frac{|z|}{h} \right] \quad (12)$$

where $R_d \sim 3.5kpc$ is in the order of disk radius and h and Σ_{\odot} represent the thickness and column density of disk respectively. In our analysis we consider two types of disk which are called thin and thick disk models. The thin disk mainly is made up by the population of stars and gas. The column density and thickness of disk in this model near the sun is about $\Sigma_{\odot} \sim 50M_{\odot}pc^{-2}$ and $h = 0.32kpc$. In the case of thick disk, dark matter contribution also is taken into account. Here, we choose

$\Sigma_{\odot} \sim 100M_{\odot}pc^{-2}$ and $h = 1kpc$. The rotational velocity of disk also is given by [17]:

$$V_{disk}(R)^2 = 4\pi G\Sigma_{\odot}R_d e^{R_{\odot}/R_d} y^2 [I_0(y)K_0(y) - I_1(y)K_1(y)], \quad (13)$$

where $y = R/(2R_d)$ and I_n and K_n are the modified Bessel functions. The velocity distribution for two models of disk is shown in Figure(1).

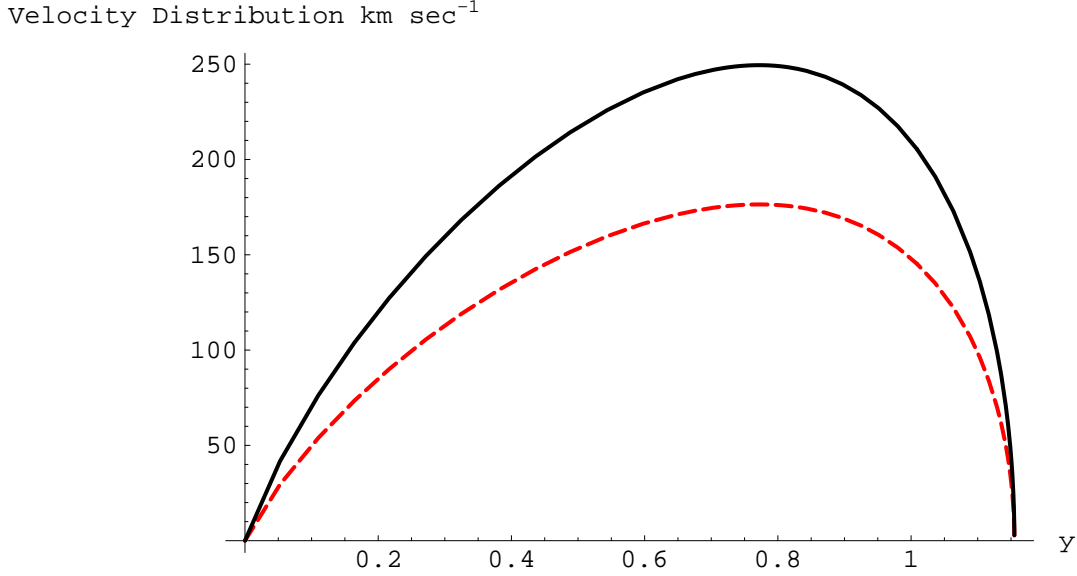


Figure 1: Thick line represents the rotational velocity of thick disk and the dashed line shows this distribution for thin disk, x-axis indicates the distance of disk from the center of galaxy in terms of $y = 2R/R_d$.

3.2 Power law halo model

The largest known set of axisymmetric model is called the "power law galaxies". The density of halo in the cylindrical coordinate system is given by:

$$\rho(R, z) = \frac{V_a^2 R_c^\beta}{4\pi G q^2} \times \frac{R_c^2(1 + 2q^2) + R^2(1 - \beta q^2) + z^2[2 - (1 + \beta)/q^2]}{(R_c^2 + R^2 + z^2/q^2)^{(\beta+4)/2}}, \quad (14)$$

where R_c is the core radius and q is the flattening parameter, which is the axis ratio of concentric equipotential. $q = 1$ represents a spherical ($E0$) halo and $q \sim 0.7$ gives an ellipticity of about $E6$. The parameter of β determines whether the rotational curve asymptotically rises, falls or is flat. At large distance R in the equatorial plane, the rotational velocity is given by $V_{circ} \sim R^{-\beta}$. Therefore $\beta = 0$ corresponds to flat the rotational curve, $\beta < 0$ is a rising rotational curve, and $\beta > 0$ is falling. The parameter V_a determines the overall depth of the potential well and hence gives the typical velocities of lenses in the halo. The density distribution in the spherical symmetric models ($q = 1$) for an observer that located at the position of sun and

observes in the line of sight of Large Magellanic Cloud ($l=280$, $b=-33$) obtain by:

$$\rho(r) = \frac{V_a^2 R_c^\beta}{4\pi G} \times \frac{3R_c^2 + (1 - \beta)[R_0^2 + r^2 - 2rR_0 \cos(l) \cos(b)]}{[R_c^2 + (1 - \beta)(R_0^2 + r^2 - 2rR_0 \cos(l) \cos(b))]^{(\beta+4)/2}}. \quad (15)$$

The velocity dispersion of lenses relate to the center of galaxy in the cylindrical coordinate system is given as follows [10]:

$$\begin{aligned} \sigma_r^2 &= \sigma_z^2 = \frac{V_a^2 R_c^\beta}{2(1 + \beta)} \frac{1}{(R_c^2 + R^2 + z^2/q^2)^{\beta/2}} \\ &\times \frac{2q^2 R_c^\beta + (1 - \beta)q^2 R^2 + z^2[2 - (1 + \beta)/q^2]}{R_c^2(1 + 2q^2) + R^2(1 - \beta q^2) + z^2[2 - (1 + \beta)/q^2]}, \end{aligned} \quad (16)$$

$$\begin{aligned} \sigma_\phi^2 &= \frac{V_a^2 R_c^\beta}{2(1 + \beta)} \frac{1}{(R_c^2 + R^2 + z^2/q^2)^{\beta/2}} \\ &\times \frac{2q^2 R_c^\beta + [2 + 2\beta - (1 + 3\beta)q^2]R^2 + z^2[2 - (1 + \beta)/q^2]}{R_c^2(1 + 2q^2) + R^2(1 - \beta q^2) + z^2[2 - (1 + \beta)/q^2]}. \end{aligned} \quad (17)$$

Like the distribution of matter, we want to obtain the velocity distribution related to the new frame at the position of sun. The distribution of transverse velocity in the lens plane which we denoted it by v_t , is given by taking integral along the line of sight. For the spherical symmetric models ($q = 1$) the transverse velocity distribution in the lens plane is

$$f(v_t)v_t dv_t = \frac{1}{\sigma^2} \exp\left(-\frac{v_t^2}{2\sigma^2}\right)v_t dv_t, \quad (18)$$

where

$$\begin{aligned} \sigma^2 &= \frac{V_a^2 R_c^\beta}{2(1 + \beta)} \frac{1}{[R_c^2 + (1 - \beta)(R_0^2 + r^2 - 2rR_0 \cos(l) \cos(b))]^{\beta/2}} \\ &\times \frac{2R_c^\beta + (1 - \beta)(R_0^2 + r^2 - 2rR_0 \cos(l) \cos(b))}{3R_c^2 + (1 - \beta)(R_0^2 + r^2 - 2rR_0 \cos(l) \cos(b))}. \end{aligned} \quad (19)$$

Here in our study, we take into account six galactic model ([18], [19] & [20]) with the following parameters:

Model 1a: standard halo and thin disk.

Model 1b: standard halo and thick disk.

Model 2a: power law model ($q=1$ and $\beta = 0$) and thin disk.

Model 2b: power law model ($q=1$ and $\beta = 0$) and thick disk.

Model 4: spherical halo with asymptotic decreasing rotational velocity ($q=1$ and $\beta = 0.2$) and thin disk.

Model 6: spherical halo with flat rotational curve ($q = 1$ and $\beta = 0$) and intermediate disk.

Table (1) shows the parameters of these models.

Unlike the Evans models, in the standard halo model (1a, 1b), the velocity dispersion of lenses in the halo is approximately independent from space and its value $\sigma = 156 \text{ km/sec}$. Figure (2) shows the transverse velocity distribution in the spherically symmetric models 2a, 2b, 4 and 6. Next section contain Monte-Carlo simulation for generating microlensing events in Evans model to evaluate the expected rate of events.

<i>Model :</i>	1a	1b	2a	2b	4	6
$\Sigma_0(M_\odot/pc^2)$	50	100	50	100	50	80
$R_d(kpc)$	3.5	3.5	3.5	3.5	3.5	3.
$R_c(kpc)$	5	5	5	5	5	15
ρ_\odot	0.008	0.008	0.008	0.003	0.007	0.005
β	-	-	0	0	0.2	0
q	-	-	1	1	1	1
V_a	-	-	165	100	170	170
$M_{Halo}(60kpc)(10^{11} M_\odot)$	5.1	5.1	1.9	0.7	1.2	2.2

Table 1: Parameters of the power law model. First part of the table represents the parameters of the disk and the second part shows the halo parameters.

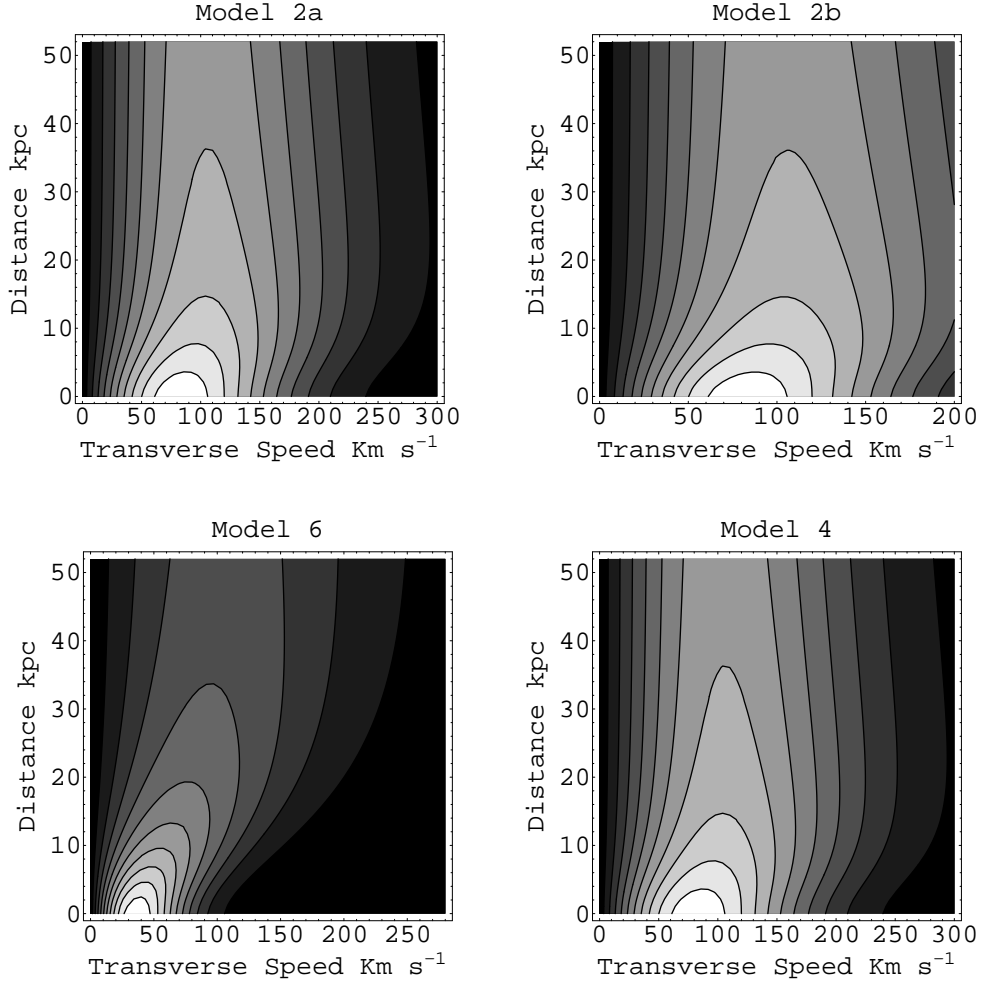


Figure 2: 2-Dimension Contours shows the distribution of transverse velocity and the distance of lenses with respect to an observer that located at the position of sun and observes the direction LMC in different Evans halo models.

4 Monte-Carlo Simulation

In this section we use Monte-Carlo simulation to obtain the theoretical distribution of events duration for each galactic models. We then apply the observational efficiency of EROS and MACHO groups to the theoretical distributions to obtain the expected distribution of events. One can compare these distributions with the observed events and the aim is to put a constraint on the fraction of halo that can be made by MACHOs. Here, we supposed that all the microlensing events are due to halo or galactic disk lenses and we ignore those located in the LMC itself (self lensing). Next generation microlensing experiments with high sampling rate and sufficient photometric precision, definitely will solve the question of self-lensing hypothesis [21].

We introduce the main functions for this Monte-Carlo simulation which are the spatial distribution of lenses, distribution of velocity and the mass function of compact objects. For the mass function of the halo, we use the power law model as follows [22]:

$$P(M)d\left(\frac{M}{M_0}\right) = A\left(\frac{M}{M_0}\right)^\alpha d\left(\frac{M}{M_0}\right), \quad \text{for } M_{min} \leq M \leq M_{max}, \quad (20)$$

where $M_0 = (M_{min}M_{max})^{1/2}$. The exponent $\alpha = -1.5$ according to the Expression (5) corresponds to an equal rate of microlensing events per decade of lens masses and also $\alpha = -2$ corresponds to an equal contribution to the optical depth per decade of less masses. In the range of $-1.5 < \alpha < -2$, the optical depth is dominated by massive objects and event rate is dominated by low mass objects. For the $\alpha < -2$ both optical depth and event rate are dominated by low massive objects, while for $\alpha > -1.5$ optical depth and event rate are dominated by massive objects. The domain for the Mass Function is defined by β :

$$\beta = \log(M_{max}/M_{min}) \quad (21)$$

Here in this simulation we choose $\alpha = -1.5$ and $\beta = 1$. One can simplify problem by identifying a mass scale. We assume such a mass scale is provided by a fixed upper mass limit, say $M_{max} = 1M_\odot$. In the case of mass function for the disk, it has been proposed by HST observations [25]. In the disk MF the slope is changed at $M \sim 0.6M_\odot$, from a near-Salpeter power-law index of $\alpha = -1.21$ to $\alpha = 0.44$. The best fit to mass function of disk indicated straight line, $d \log N/d \log M = -1.37 - 1.21 \log(\frac{M}{M_\odot})$ for $M > 0.6M_\odot$ and $d \log N/d \log M = -0.99 + 0.44 \log(\frac{M}{M_\odot})$ for $M < 0.6M_\odot$.

Figure (3) shows the observed mass function by HST.

The spatial distribution of lenses obtain along our line of sight by Eq. (5)

$$\text{probability of observation} \propto \rho(x)\sqrt{x(1-x)}.$$

Using the different galactic models mentioned in Table.(1), the spatial distribution of lenses along our line of sight obtain according to Figures (4 & 5).

Here is the algorithm that we use in this simulation:

We start from the distance of the lenses from the observer via the distance distributions, in Figures.(4 & 5). The mass of MACHOs obtain according to the mass functions of the Halo and disk. Combing the distance and the mass of the lens by Eq. (2) yields the corresponding Einstein radius of the lens. The transverse velocity distribution also depending on the galactic models, has been obtained in Figures (1

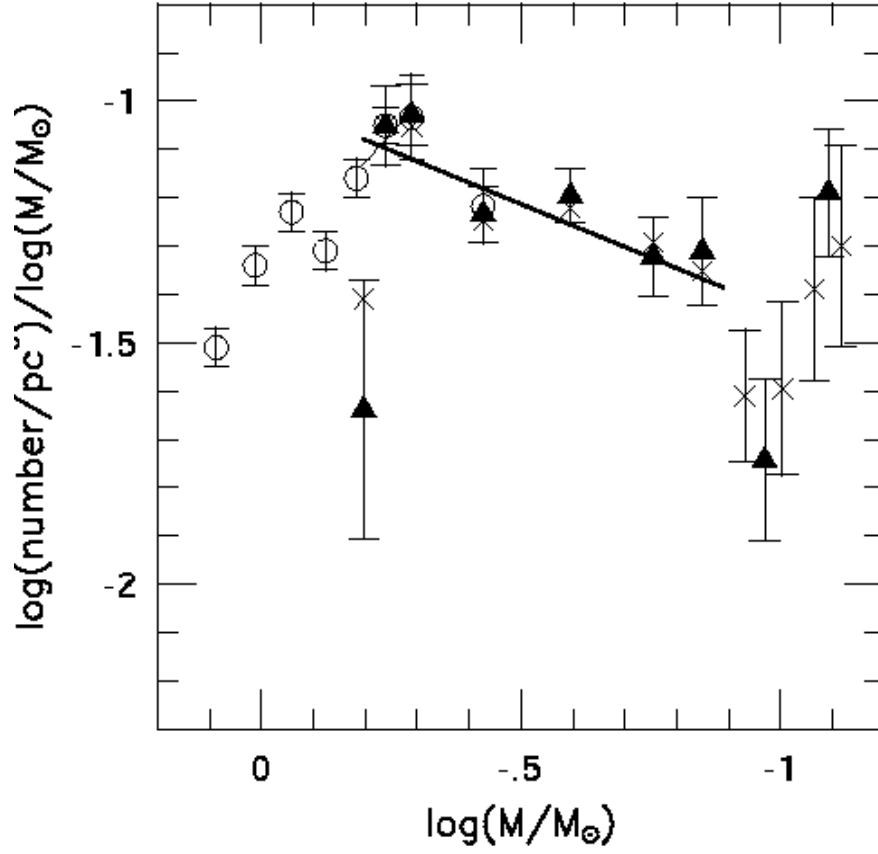


Figure 3: The mass function of disk [25]. The slope of the MF changes near the $M \sim 0.6M_{\odot}$, from a near-Salpeter power-law index of $\alpha = -1.21$ to $\alpha = 0.44$.

Distribution of Lens

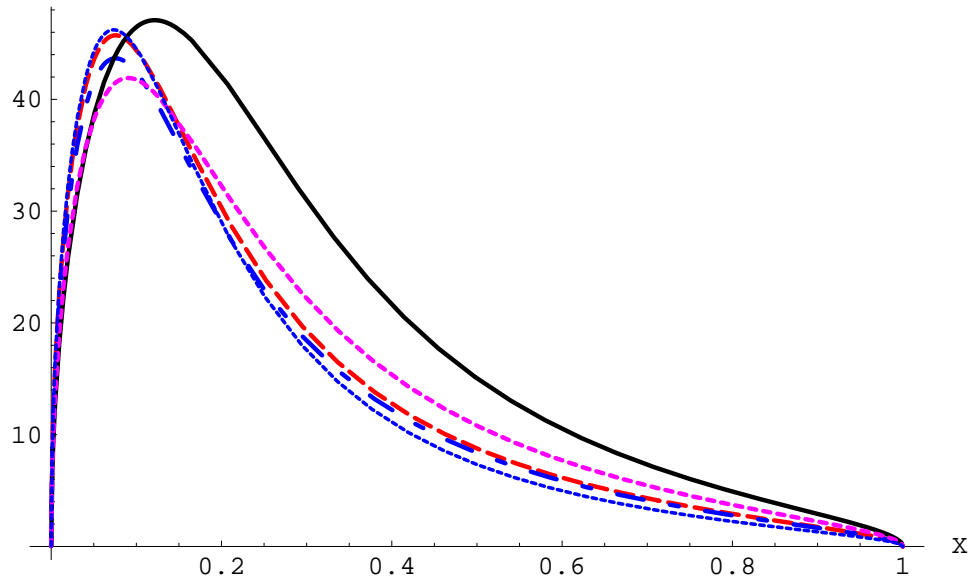


Figure 4: The distribution of lenses as function of distance from the observer in the different galactic halo models. dot-line stands for standard halo, dot-thin line for model 4, thick line for model 6, dot-dashed line for model 2b and dashed line represents model 2a.

Distribution of Lens

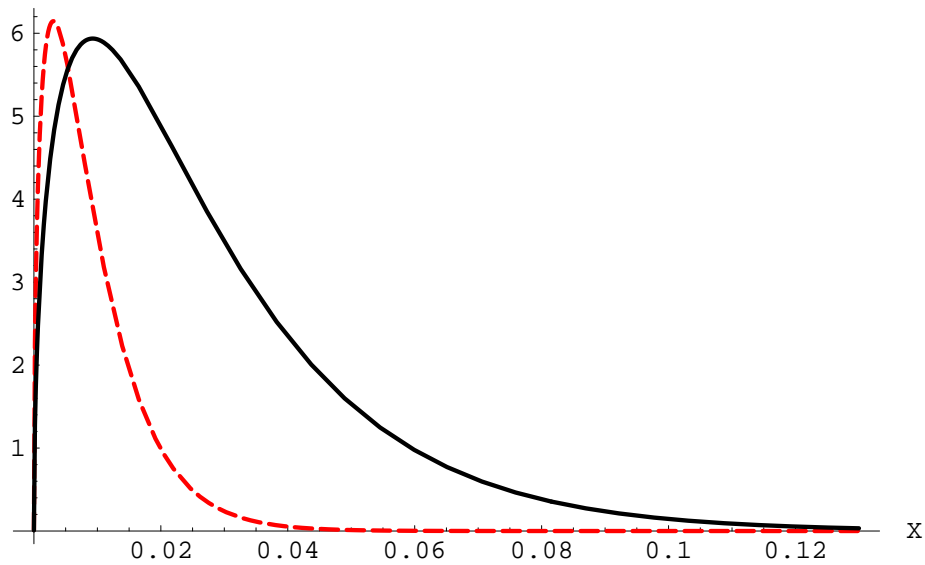


Figure 5: The distribution of lenses as function of distance from the observer in the different disk models. Solid-line represents this distribution in thick disk model and dashed line shows thin disk model.

& 2). We use the transverse velocity of the lens and its Einstein radius to calculate the duration of events by following formula:

$$t_E = 78.11 \left(\frac{M}{M_\odot} \right)^{1/2} \left(\frac{D_s}{10kpc} x(1-x) \right)^{1/2} \left(\frac{200km/s}{v_t} \right) \text{ days} \quad (22)$$

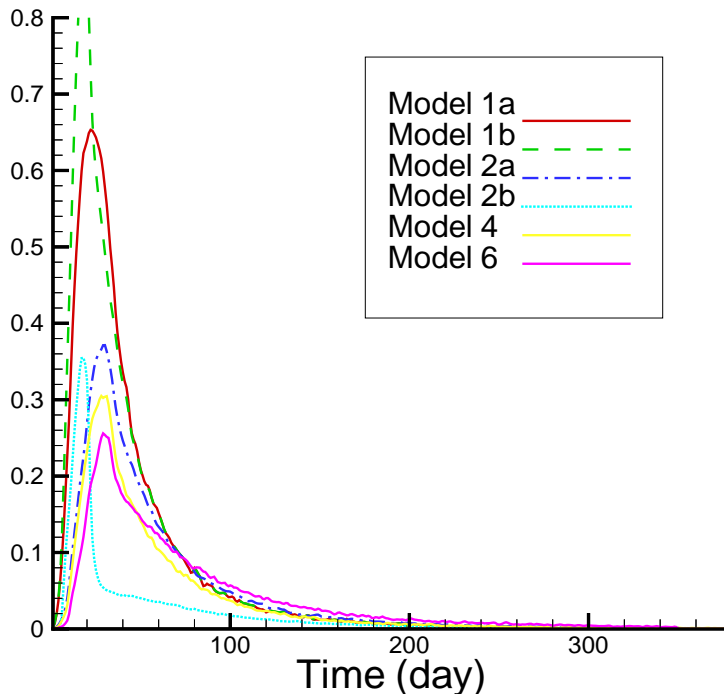


Figure 6: The distribution of events verses duration of events for different galactic models. The total number of events are normalized with the rate of events in one year for 10^7 background stars which obtained by Table 2.

Figure (6) shows the distribution of events for different galactic models, where the number of events are normalized $10^7 \text{ star} \times \text{yr}$ exposure time with 100 percent efficiency in observation. The normalization have been done by Eq. (10), using the numerical optical depth value and the mean of inverse Einstein crossing time.¹ Here we assume that hundred percent of halo is made by compact halo objects. Table (2) as result of simulation shows corresponding optical depth and the rate of events in galactic models. To obtain quantitative conclusion, we clearly need to assess our event detection efficiency. The detection probability for individual events is complication function of u_0 , t_E , the strategy of observation and the brightness of the source stars. In fact all these distributions except t_E are not known and thus can be averaged over by a Monte-Carlo simulation. Here we use the observational efficiency of EROS and MACHO experiments in our simulation. The detection efficiency of MACHO group in the term of event duration can be found in [23] and for the EROS group in [24]. For the efficiency calculation in EROS group, microlensing

¹We used THalo code developed in EROS for optical depth calculation

Table 2: Optical depth and the rate of microlensing events is given toward LMC for each elements of galactic structure.

<i>Model :</i>	1a	1b	2a	2b	4	6
$\tau_{Halo}(LMC)10^{-7}$	4.96	4.96	3.92	1.44	2.82	3.58
$\tau_{Disk}(LMC)10^{-7}$	0.19	0.39	0.19	0.39	0.19	0.31
$\tau_{Total}(LMC)10^{-7}$	5.15	5.35	4.11	1.83	3.1	3.89
$\Gamma_{Halo}(/10^7 starYr)(LMC)$	41.5	41.5	18.21	5.53	16.38	15.
$\Gamma_{Disk}(/10^7 starYr)(LMC)$	2.20	4.40	2.20	4.40	2.20	3.52
$\Gamma_{Total}(/10^7 starYr)(LMC)$	43.69	45.89	20.41	9.93	18.58	18.52

parameters are drawn uniformly in the following intervals: time of maximum magnification t_0 within the observing period $\pm 150 days$, impact parameter normalized to Einstein radius $u_0 \in [0, 2]$ and time scale $t_E \in [5, 300] days$ [24], where the efficiency is normalized to events with the impact parameters $u_0 < 1$. The Efficiency of these two groups are shown in Figure. (7). It should be mentioned that the conventional definition of Einstein crossing time by EROS is the half of its value defined by MACHO group, here by convention we follow the time scale definition according to equation (22).

The expected distribution of events can be obtained by multiplying the efficiency to the theoretical distribution of $d\Gamma/dt_E$. The expected observation is shown in Figure (8). Table (3) indicates overall expected number of events by EROS and MACHO for 10^7 time-object exposure in each galactic models. The Constraint on the contribution of the compact objects in the dark matter of halo obtain by comparing the number of microlensing candidates with those expected from galactic models. Here we use two different statistical approach for analyzing EROS and MACHO data.

EROS observed two candidates during $2 year$ observations of 17.5 million stars in LMC [26]. The microlensing candidates were called EROS-LMC-3 and 4 with Einstein crossing time in 41 and 106 days. Now, for statistical analysis, let b is the total expected number of events for a given galactic model (Table 3) and n_0 be the observed events in the absence of background. Considering the Poisson probability distribution for events, one can obtain Poisson confidence intervals $[\mu_1, \mu_2]$ for n_0 observed events. In particular case we want to put an upper limit for b with a certain level of confidence. For instance, observing two events by EROS allows us to put a constraint, excluding at 95% C.L that the expected number of events should not be more than 6.72, let call this number "C". To compare this number with Table. 3 we normalize the numbers of table to the exposure time of EROS, $(2 \times 17.5 \times 10^6 year * star)$. The fraction of halo that made by MACHOs can be obtained by $f_M < C/F_M$ (at 95%CL), where the F_M is the expected number of events in the Table. (3), taking into account the normalization factor. The results for EROS indicated in Table (4). It is seen that except the minimal halo model, the compact objects form a fraction of halo mass.

The analysis of 5.7 year of photometric on 11.9 million stars by MACHO group in the LMC also reveals 13-17 microlensing events [12]. We normalize the rate of events in the Table (3) to the exposure time of MACHO, $(5.7 \times 11.9 \times 10^6 star \times year)$. For the statistical analyzing of MACHO results, unlike the former approach used for EROS results, here we consider the part of halo mass that is allowed to be in the form of MACHOs with one sigma error. This fraction obtain by dividing (13 – 17)

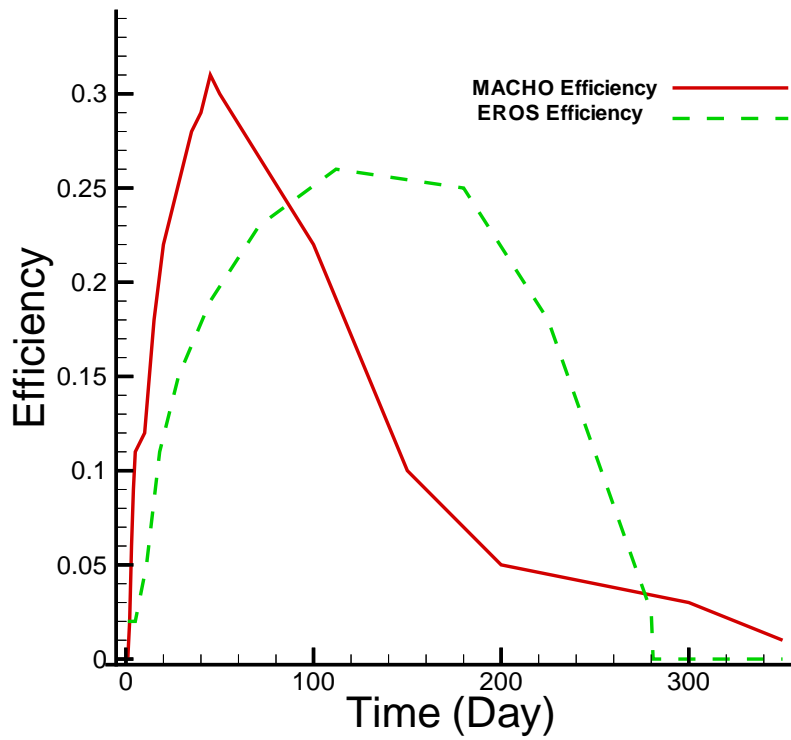


Figure 7: Detection efficiency verses event duration t_E toward LMC. The solid line shows the efficiency of MACHO [23] and dashed line indicates for EROS group [24].

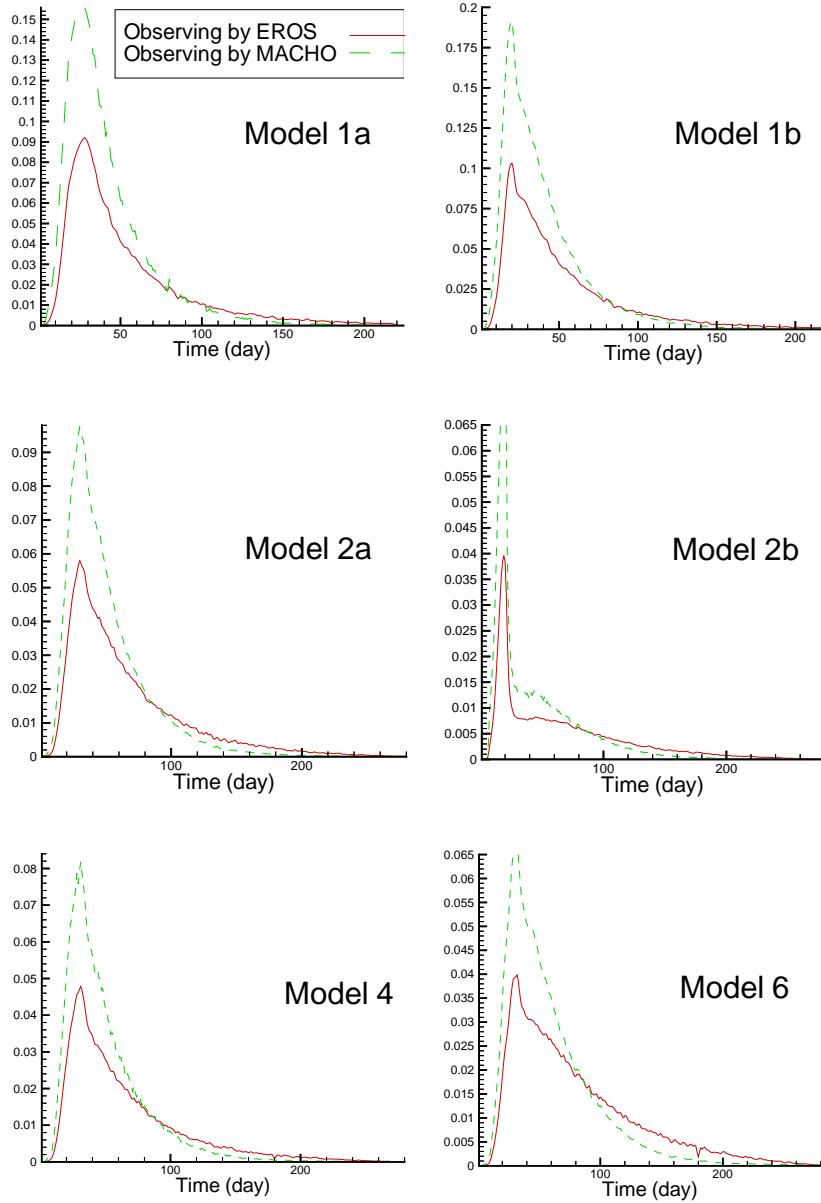


Figure 8: The distributions of events versus duration are shown for different galactic models. The total number of events are normalized by Table (2) with the exposure time of 10^7 background stars in one year.

Table 3: EROS/MACHO expected number of microlensing events, considering that 100% of halo made by compact objects are obtained in $10^7 \text{star} \times \text{yr}$ exposure time.

<i>Model</i> :	<i>1a</i>	<i>1b</i>	<i>2a</i>	<i>2b</i>	<i>4</i>	<i>6</i>
EROS	6.81	6.93	3.64	1.59	3.29	3.23
MACHO	10.1	10.43	4.84	2.02	4.39	3.82

Table 4: The fraction of halo in the form of MACHO obtain by comparing the observational results of experiments with the expected theoretical number of events. This fraction depends on galactic model and the mass function of compact halo objects. The EROS results obtain by excluding f_{EROS} with 95%*C.L* to be less than indicated value. MACHO results have also been obtained with one sigma error for f_{MACHO} .

<i>Model</i> :	<i>1a</i>	<i>1b</i>	<i>2a</i>	<i>2b</i>	<i>4</i>	<i>6</i>
$f_{EROS} <$	0.28	0.27	0.52	1.	0.58	0.59
f_{MACHO}	$0.25^{+0.06}_{-0.06}$	$0.24^{+0.05}_{-0.05}$	$0.52^{+0.12}_{-0.12}$	1	$0.57^{+0.14}_{-0.14}$	$0.66^{+0.16}_{-0.16}$

events to the normalized number of events in Table. (3). The results indicated in Table. (4).

5 Conclusion

Two years observation of Large Magellanic Clouds by EROS and 5.7 years by MACHO, revealed 2 and (13 – 17) microlensing candidates, respectively. The results presented here provide some interesting conclusion on the contribution of MACHOs in the halo of our galaxy, depending on the models.

It is seen that except minimal halo model, the number of observed events are inadequate that halo fully comprised of $[0.1, 1]M_{\odot}$ compact halo objects. Two extreme results are considering a non spherical halo (minimal halo) and another possibility is an LMC halo that dominate microlensing, and no MACHOs in the Milky Way. The essential way to distinguish the real model of our galaxy and the contribution of compact objects on the halo is localizing the position of lenses. Studying parallax, finite size effect and double lenses would allow us to achieve this aim. Recently, analysis of MACHO-99-BLG-22/OGLE-1999-BUL-32, indicated parallax effect in its light curve. A likelihood analysis of the lens position implies that lens could be a black hole [27] & [28]. The analysis of PLANET photometric observations of event EROS BLG-2000-5 ² shows the parallax and binary orbital motion in its light curve. It is the first time that the lens mass degeneracy have been completely broken [29]. In spite of localizing some events toward galactic bulge, in the direction of LMC, the position of lenses have not been localized and it needs next generation microlensing experiments with high sampling rate and better photometric precision [21].

The fraction of halo (derived from microlensing experiments) in the form of MACHOs can also be compared with the White Dwarf [30] & [31] population from the

²<http://www-dapnia.cea.fr/Spp/Experiences/EROS/aletts.html>

Hubble Deep Field. Although the identification of these faint blue objects as white dwarfs remains to be confirmed and the small sample size restricts an accurate estimate, the suggestion that these White dwarfs could contribute 1/3 to 1/2 of the dark matter in the Milky Way. This result is in agreement with the fraction of halo in the form of compact objects in some of halo models. The galactic halo, composed of White Dwarfs would seem to be a natural explanation of the microlensing data.

References

- [1] Faber, S. M., Gallagher J. S., 1979, *Ann. Rev. Astron. Astrophys* 17, 135.
- [2] Trimble, V., 1987, *Ann. Rev. Astron. Astrophys* 25, 425.
- [3] Persic, M., Salucci, P and Stel, F., 1996, *MNRAS* 281, 27.
- [4] Moore, B., 1994, *Nature* 370, 629.
- [5] Navarro, J. F., Frenk, C. S., White, S. D., 1996, *APJ* 462, 563.
- [6] Copi, C. J., Schramm, D. N and Turner, M. S., 1995, *Science* 267, 192.
- [7] Burles, S., Tyler, D., 1998, *APJ* 499, 699.
- [8] Fukugita M., Hogan C. J., Peebles P. J. E., 1995, *A&A* 503, 518.
- [9] Paczyński B., 1986, *APJ* 304, 1.
- [10] Evans N. W., 1994, *MNRAS* 267, 333.
- [11] Spiro M., Lasserre T, *Cosmology and Particle Physics*, edited by Durrer, R., Garcia-Bellido, J and Shaposhnikov, M (American Intitute of Physics),(2001) 146.
- [12] Alcock C. et al. (MACHO)., 2000, *APJ* 542, 281.
- [13] Paczyński B., 1996, *Annu. Rev. Astron. Astrophys* 34, 419.
- [14] Roulet E., Mollerach S., 1997, *Phys. Rep* 279, 67.
- [15] Gould A, *A New Era of Microlensing Astrophysics*, edited by Menzies J. W., Sackett P. D., (ASP conference Series), preprint (astro-ph/0004042).
- [16] Jetzer P., 1997, *Proceeding of 8th Marcel Grossmann Meeting on Relativistic Astrophysics*, Jerusalem, preprint (astro-ph/9709212).
- [17] Binney S., Tremaine S *Galactic Dynamics*. Princeton University Press (1987).
- [18] Alcock C. et al. (MACHO), 1995, *APJ* 449, 28.
- [19] Renault C., PhD thesis, Université, Paris 7, DAPNIA/SPP 96-1003, (pub no. 96001264)
- [20] Palanque-Delabrouille, PhD thesis, University Paris 7 and University of Chicago, DAPNIA/SPP 97-1007
- [21] Rahvar S., Moniez M., Ansari R., Perdereau O., 2002 (submitted in A&A).
- [22] Mao S., Paczynski B., 1996, *APJ* 473, 57.
- [23] Sutherland W., 1999, *Rev. Mod. Phys.* 71, 421.
- [24] Palanque-Delabrouille N. et al. (EROS)., 1998, *A&A* 332, 1.
- [25] Gould A., Bahcall J. N., Flynn C., 1997, *APJ* 482, 913.
- [26] Lasserre T. et al. (EROS)., 2000, *A&A* 355, 39.

- [27] Bennett, D. P. *et al*, preprint (astro-ph/0207006).
- [28] Mao, S. *et al*, 2002, MNRAS, 329, 349.
- [29] An, J. *et al*, 2002, APJ, in press (astro-ph/0110095).
- [30] Ibata, R. A. *et al*, 1999, APJ 524, 1.
- [31] Méndez, R. A and Minniti, D., 2000, APJ 529, 911.